# Novel Structural Modulation in the Ambient-Pressure Sulfur-Based Organic Superconductor $\beta$-(BEDT-TTF)$_2$I$_3$: Origin and Effects on Its Electrical Conductivity

**Peter C. W. Leung,[†] Thomas J. Emge,[†] Mark A. Beno,[†] Hau H. Wang,[†] Jack M. Williams,*[†] Vaclav Petricek,[†§3] and Philip Coppens[‡]**

*Contribution from the Chemistry and Materials Science and Technology Divisions, Argonne National Laboratory, Argonne, Illinois 60439, and the Chemistry Department, State University of New York at Buffalo, Buffalo, New York 14214.* *Received April 10, 1985*

**Abstract:** The organic charge-transfer complex, $\beta$-(BEDT-TTF)$_2$I$_3$ [BEDT-TTF is bis(ethylenedithio)tetrathiafulvalene, ($C_{10}S_8H_8$)], is the first ambient-pressure sulfur-based organic superconductor ($T_c$ = 1.4 (1) K). The space group for this material is $P\bar{1}$ ($Z$ = 1) and the unit cell parameters (120 K) are the following: $a$ = 6.560 (1) Å, $b$ = 9.011 (2) Å, $c$ = 15.171 (3) Å, $\alpha$ = 95.08 (2)°, $\beta$ = 95.94 (2)°, $\gamma$ = 110.28 (2)°, and $V_c$ = 829.2 (3) Å$^3$. Evidence of an incommensurate structural modulation is observed from the appearance of satellite reflections at temperatures below 195 K. For each fundamental Bragg reflection, there are two first-order satellite reflections which are symmetrically displaced about the main reflection by the vector $\pm\mathbf{q}$ = [0.076 (2)]$\mathbf{a}^*$ + [0.272 (4)]$\mathbf{b}^*$ + [0.206 (3)]$\mathbf{c}^*$. The narrow full-width at half-height (fwhh) values of these satellite reflections at low temperatures suggests long-range order in the modulated structure. A full structural determination of this material utilizing a four-dimensional space group and complete (fundamental and satellite) reflection data collected at 120 K was undertaken. A significant feature of the basic structure at 120 K is the two-dimensional (2-D) network of the BEDT-TTF molecules, which is characterized by very short *inter*stack S···S contacts (<3.6 Å) between adjacent molecules. This 2-D "corrugated sheet" network of S···S interactions is largely responsible for the anisotropic electronic properties of this organic metal. Although the structural modulation results in significant fluctuations of the S···S contacts (up to ±0.2 Å from the average), the two-dimensional cationic network is preserved, which is in agreement with the observation that $\beta$-(BEDT-TTF)$_2$I$_3$ remains metallic below the incommensurate structural phase transition temperature. The origin of this incommensurate phase transition in this material is a result of H···I type crystal packing interactions between the BEDT-TTF molecules and the triiodide anions. The structural modulation results in long-range ordering of one of the two ethylene groups in each BEDT-TTF molecule which is otherwise disordered at 298 K.

In recent years, a number of organic radical cations have been found to form metallic charge-transfer salts with either organic or inorganic anions. The earliest of these so-called "organic metals", (perylene) $Br_x$, was first reported in 1954.[1] Research on a variety of organic conductors intensified after the discoveries of the $\pi$ acceptor tetracyano-*p*-quinodimethane (TCNQ)[2] and the sulfur based $\pi$ donor tetrathiafulvalene (TTF).[3] The charge-transfer salt derived from these two materials, TTF-TCNQ, is metallic in nature, and its electrical conductivity has been reported to be as high as $10^4$ $\Omega^{-1}$cm$^{-1}$ at ~54 K.[4,5] In TTF-TCNQ, the partial charge transfer and extensive $\pi$ overlap between adjacent molecules in the cation (TTF) or anion (TCNQ) columns produce a high degree of *intra*chain electronic delocalization and high electrical conductivity in the stacking direction.

As a result of weak interactions between the segregated stacks, which is characteristic of many one-dimensional (1-D) conductors, the electrical conductivity of TTF-TCNQ is highly anisotropic and susceptible to structural distortions from electronic instabilities. This material is metallic for $T$ > 54 K, at which temperature a Peierls distortion occurs. Below this temperature, a crystallographic instability (crystal lattice distortion) occurs and is accompanied by a rapid decrease in electrical conductivity.[4,5]

Another major advance in organic metal research came with the discovery of superconductivity in (TMTSF)$_2$PF$_6$ (TMTSF (**1**) is tetramethyltetraselenafulvalene, a derivative of TTF) under hydrostatic pressure ($P_c$ ~ 12 kbar, $T_c$ ~ 0.9 K).[6] Shortly thereafter, superconductivity was observed in the derivatives of (TMTSF)$_2$X, X = $PF_6^-$, $AsF_6^-$, $SbF_6^-$, $TaF_6^-$, $ReO_4^-$, and $ClO_4^-$.[7] With the exception of the $ClO_4^-$ salt which was the sole ambient pressure organic superconductor known at that time,[8] all of these materials undergo metal-insulator transitions (MI) at low temperature and ambient pressure and are superconducting only under hydrostatic pressure in the ~10-kbar range.[7] By contrast, superconductivity has not yet been observed in the isoelectronic and isostructural (TMTTF)$_2$X series (TMTTF (**2**) is tetramethyltetrathiofulvalene) even under high pressure.[9]

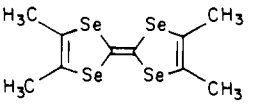

TMTSF (**1**)

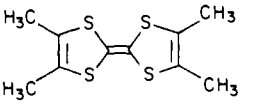

TMTTF (**2**)

Following the discovery of superconductivity in the (TMTSF)$_2$X systems, research in this field quickly diverged into studies of other potential organic donors. The discovery of superconductivity in the first sulfur-based organic metal (BEDT-TTF)$_2$ReO$_4$ soon followed.[10] BEDT-TTF, bis(ethylenedithio)tetrathiafulvalene (**3**, $C_{10}S_8H_8$, also commonly referred to as "ET"), is a sulfur-based derivative of TMTTF. As is the case for many TMTSF salts,

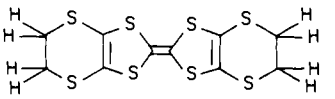

BEDT-TTF or "ET" (**3**)

[†] Argonne National Laboratory.
[‡] State University of New York at Buffalo.

(1) Akamatu, H.; Inokuchi, H.; Matsunaga, Y. *Nature (London)* **1954**, *173*, 168.
(2) Acker, D. S.; Harder, R. J.; Hertler, W. R.; Mahler, W.; Melby, L. R.; Benson, R. E.; Mochel, W. E. *J. Am. Chem. Soc.* **1960**, *82*, 6048.
(3) Wudl, F.; Smith, G. M.; Hufnagel, E. J. *J. Chem. Soc., Chem. Commun.* **1970**, 1453.
(4) Ferraris, J.; Cowan, D. O.; Walatka, V. V., Jr.; Perlstein, J. H. *J. Am. Chem. Soc.* **1973**, *95*, 948.
(5) Coleman, L. B.; Cohen, M. J.; Sandman, D. J.; Yamagishi, F. G.; Garito, A. F.; Heeger, A. J. *Solid State Commun.* **1973**, *12*, 1125.
(6) Jerome, D.; Mazaud, A.; Ribault, M.; Bechgaard, K. *J. Phys. Lett. (Paris)* **1980**, *41*, L195.
(7) Bechgaard, K. *Mol. Cryst. Liq. Cryst.* **1982**, *79*, 1 and references therein.
(8) Bechgaard, K.; Carneiro, K.; Rasmussen, F. B.; Olsen, M.; Rindorf, G.; Jacobsen, C. S.; Pedersen, H. J.; Scott, J. C. *J. Am. Chem. Soc.* **1981**, *103*, 2440.
(9) Coulon, C.; Delhaes, P.; Flandrois, S.; Lagnier, R.; Bonjour, E.; Fabre, J. M. *J. Phys. (Les Ulis, Fr.)* **1982**, *43*, 1059.
(10) Parkin, S. S. P.; Engler, E. M.; Schumaker, R. R.; Lagier, R.; Lee, V. Y.; Scott, J. C.; Greene, R. L. *Phys. Rev. Lett.* **1983**, *50*, 270.

0002-7863/85/1507-6184$01.50/0 

pressure is required to achieve superconductivity ($T_c \simeq 2$ K, $P > 4$ kbar) and to suppress the metal-insulator transition which otherwise occurs at 81 K under ambient pressure in $(ET)_2ReO_4$.

Numerous $(ET)_2X$ charge-transfer salts, X = monovalent anion, have been synthesized and observed to have vastly different electrical properties which range from metallic to semiconducting to insulating.[11,12] The first *ambient pressure* sulfur-based organic superconductor is the charge-transfer salt, $\beta$-$(ET)_2I_3$, discovered by Yagubskii et al.[13] and confirmed in two independent studies.[14-16] Unlike $(ET)_2ReO_4$, when this material is cooled it remains metallic to 1.4 K at ambient pressure, at which temperature the onset of superconductivity occurs. The MI transition commonly observed in other organic metals is not observed in $\beta$-$(ET)_2I_3$, probably because of the electronic structure arising from the 2-dimensional (2-D) nature of the packing of the ET molecules, namely, the network of S···S interactions in the crystal.[16-18] Another charge-transfer salt also cocrystallizes with $\beta$-$(ET)_2I_3$ [designated as $\alpha$-$(ET)_2I_3$].[16,19] Although the crystal packing motifs of the two forms are different, $\alpha$-$(ET)_2I_3$ also exhibits 2-D metallic properties.[19] However, an MI transition occurs in $\alpha$-$(ET)_2I_3$ at ~135 K under ambient pressure.

Unlike previously studied organic metals that undergo structural changes during an MI transition, $\beta$-$(ET)_2I_3$ exhibits a structural transition[21,30] *without* a significant change in its electrical behavior (i.e., the resistivity displays no abrupt change near $T \simeq 200$ K).[20] At temperatures below ~200 K, satellite reflections that are incommensurate with the fundamental lattice are observed with both X-ray (120 K) and neutron (20 K) diffraction data.[21] There are two first-order satellite reflections, symmetrically displaced by the vector $\pm\mathbf{q} = 0.076\,\mathbf{a}^* + 0.272\mathbf{b}^* + 0.206\mathbf{c}^*$ about each fundamental Bragg reflection. These incommensurate satellite reflections are indicative of a sinusoidal structural modulation. The full-width at half-height (fwhh) values of the satellite reflections, which converged quickly to the instrumental resolution limit below 195 K, suggested long-range structural order in the modulated structure at $T < 195$ K. These satellite reflections are also observed in the X-ray diffuse scattering (XDS) data for $\beta$-$(ET)_2I_3$.[22] Additionally, the 195 K phase transition is accompanied by an anomaly in the thermoelectric power of this material.[23]

Incommensurate crystallographic phase transitions have been observed in various systems but never before in an organic superconductor. The transitions in TTF-TCNQ[24] and $K_2Pt(CN)_4Br_{0.3}\cdot 2D_2O$[25] are attributed to Peierls distortions[26] that are driven by charge density wave formation. Intermolecular hydrogen bonding in the charge transfer salt phenothiazine–TCNQ[27] has been identified as the driving force for its observed structural modulation. Incommensurate phase transitions are also observed in many nonconducting materials such as biphenyl[28] and $Na_2CO_3$.[29]

In a preliminary study of the incommensurate crystal structure of $\beta$-$(ET)_2I_3$ at 125 K, the triiodide anion and the ET molecule were observed to displace sinusoidally from their respective average positions in the unit cell.[30] The purpose of the present study is to identify the origin of this displacive structural modulation and its effects on the 2-D network of the ET molecules.

**Table I.** Crystallographic Data for $\beta$-$(ET)_2I_3$

| | | |
|---|---|---|
| space group, $Z$ | $P\bar{1}$, 1 | $P\bar{1}$, 1 |
| temp, K | 298 | 120 |
| $a$, Å | 6.615 (1) | 6.560 (1) |
| $b$, Å | 9.100 (1) | 9.011 (2) |
| $c$, Å | 15.286 (2) | 15.171 (3) |
| $\alpha$, deg | 94.38 (1) | 95.08 (2) |
| $\beta$, deg | 95.59 (1) | 95.94 (2) |
| $\gamma$, deg | 109.78 (1) | 110.28 (2) |
| $V$, Å$^3$ | 855.9 (2) | 829.2 (3) |
| density (calcd), g cm$^{-3}$ | 2.23 | 2.30 |
| diffractometer | | Syntex $P2_1$ |
| radiation | | Mo K$\alpha$ ($\lambda$ = 0.71073 Å) |
| monochromator | | graphite |
| data collection mode | | $2\theta$–$\theta$ scan |
| $2\theta$ range, deg | | 3–55° ($-h,\pm k,\pm l$) |
| transmission factors | | 0.57–0.68 |
| $\mu$, cm$^{-1}$ | | 37.86 |
| total no. of observations | | 10220 |
| no. of unique reflectns | | 7782 |
| fundamental reflctns | | 2702 |
| satellite reflctns | | 5080 |
| $R(F)$, $R(wF)$[a] | | 0.035, 0.022 |

[a] Agreement factors of data averaging. $R(F) = \sum|F - F_{mean}|/\sum|F|$; $R(wF) = (\sum w(F - F_{mean})^2/\sum wF^2)^{1/2}$.

## Displacive Crystal Structure Modulation

An incommensurately modulated crystal structure can be mathematically described in four-dimensional space in a manner recently described by de Wolff, Janner, and Janssen.[31] One can consider that the "average" or basic crystal structure in three-dimensional space is modulated by a sinusoidal wave. For an incommensurate phase, the wave has a period which is not a simple multiple of the basic lattice vectors. In the case of a commensurate superlattice (e.g., $a$, $2b$, $c$), the modulating wave has a period that is an integral multiple of the lattice constant (e.g., $2b$). In either case, the atoms or molecules "riding" on this wave are displaced from their mean positions in the so-called average structure.

The formalism described above was implemented recently by Coppens and co-workers[32] into a conventional least-squares structural refinement program which allows the refinement of the local molecular displacement parameters in a modulated structure. Each molecule in a crystal is assumed to be a rigid body such that

(11) Kobayashi, H.; Kato, R.; Mori, T.; Kobayashi, A.; Sasaki, Y.; Saito, G.; Enoki, T.; Inokuchi, H. *Mol. Cryst. Liq. Cryst.* **1984**, *107*, 33.
(12) Leung, P. C. W.; Beno, M. A.; Emge, T. J.; Wang, H. H.; Bowman, M. K.; Firestone, M. A.; Sowa, L. M.; Williams, J. M. *Mol. Cryst. Liq. Cryst.* **1985**, *125*, 113 and references therein.
(13) Yagubskii, E. B.; Shchegolev, I. F.; Laukhin, V. N.; Kononovich, P. A.; Kartsovnik, M. V.; Zvarykina, A. V.; Buravov, L. I. *Pis'ma Zh. Eksp. Teor. Fiz.* **1984**, *39*, 12. [*JETP Lett.* **1984**, *39*, 12].
(14) Schwenk, H.; Heidmann, C.; Gross, F.; Hess, E.; Andres, K.; Schweitzer, D.; Keller, H. *Phys. Rev. B: Condens. Matter* **1985**, *B31*, 3138.
(15) Crabtree, G. W.; Carlson, K. D.; Hall, L. N.; Copps, P. T.; Wang, H. H.; Emge, T. J.; Beno, M. A.; Williams, J. M. *Phys. Rev.* B: *Condens. Matter* **1984**, *B30*, 2958.
(16) Williams, J. M.; Emge, T. J.; Wang, H. H.; Beno, M. A.; Copps, P. T.; Hall, L. N.; Carlson, K. D.; Crabtree, G. W. *Inorg. Chem.* **1984**, *23*, 2558.
(17) Kaminskii, V. F.; Prokhorova, T. G.; Shibaeva, R. P.; Yagubskii, E. B. *Pis'ma Zh. Eksp. Teor. Fiz.* **1984**, *39*, 15 [*JETP Lett.*, **1984**, *39*, 17].
(18) Mori, T.; Kobayashi, A.; Sasaki, Y.; Kobayashi, H.; Saito, G.; Inokuchi, H. *Chem. Lett.* **1982**, 1963.
(19) Bender, K.; Hennig, I.; Schweitzer, D.; Dietz, K.; Endres, H.; Keller, H. J. *Mol. Cryst. Liq. Cryst.* **1984**, *108*, 359.
(20) Carlson, K. D.; Crabtree, G. W.; Hall, L. N.; Copps, P. T.; Wang, H. H.; Emge, T. J.; Beno, M. A.; Williams, J. M. *Mol. Cryst. Liq. Cryst.* **1985**, *119*, 357.
(21) Emge, T. J.; Leung, P. C. W.; Beno, M. A.; Schultz, A. J.; Wang, H. H.; Sowa, L. M.; Williams, J. M. *Phys. Rev. B: Condens. Matter* **1984**, *B30*, 6780.
(22) Mortensen, K., private communication (1984).
(23) Mortensen, K.; Jacobsen, C. S.; Bechgaard, K.; Carneiro, K.; Williams, J. M. *Mol. Cryst. Liq. Cryst.* **1985**, *119*, 401.
(24) Denoyer, F.; Comes, R.; Garito, A. F.; Heeger, A. J. *Phys. Rev. Lett.* **1975**, *35*, 445.
(25) Eagen, C. F.; Werner, S. A.; Saillant, R. B. *Phys. Rev. B: Condens. Matter* **1975**, *B12*, 2036.
(26) Peierls, R. E. "Quantum Theory of Solids"; Clarendon: Oxford, 1964; Chapter 5.
(27) Kobayashi, H. *Acta Crystallogr., Sect. B* **1974**, *B30*, 1010.
(28) Baudour, J. L.; Sanquer, M. *Acta Crystallogr., Sect. B* **1983**, *B39*, 75.
(29) Van Aalst, W.; Den Hollander, J.; Peterse, W. J. A. M.; De Wolff, P. M. *Acta Crystallogr., Sect. B* **1976**, *B32*, 47.
(30) Leung, P. C. W.; Emge, T. J.; Beno, M. A.; Wang, H. H.; Williams, J. M.; Petricek, V.; Coppens, P. *J. Am. Chem. Soc.* **1984**, *106*, 7644.
(31) (a) De Wolff, P. M. *Acta Crystallogr., Sect. A* **1974**, *A30*, 777. (b) Janner, A.; Janssen, T. *Phys. Rev.* **1977**, *15*, 643. (c) Janner, A.; Janssen, T. *Acta Crystallogr., Sect. A* **1980**, *A36*, 399. (d) De Wolff, P. M.; Janssen, T.; Janner, A. *Acta Crystallogr., Sect. A* **1981**, *A37*, 625. (e) Janner, A.; Janssen, T.; De Wolff, P. M. *Acta Crystallogr., Sect. A* **1983**, *A39*, 658. (f) Janner, A.; Janssen, T.; De Wolff, P. M. *Acta Crystallogr., Sect. A* **1983**, *A39*, 667. (g) Janner, A.; Janssen, T.; De Wolff, P. M. *Acta Crystallogr., Sect. A* **1983**, *A39*, 671.
(32) Petricek, V.; Coppens, P.; Becker, P. *Mol. Cryst. Liq. Cryst.* **1985**, *125*, 393.

**Table II.** Atomic Positional (Fractional Coordinates × $10^4$) and Thermal Parameters (in $Å^2 \times 10^2$)[a] for $\beta$-$(ET)_2I_3$ at 120 K

| atom | x | y | z | $U_{equiv}$[b] |
|---|---|---|---|---|
| I(1) | 0 | 0 | 0 | 1.69 (3) |
| I(2) | 4098 (1) | 2509 (1) | −187 (1) | 2.10 (3) |
| S(1) | 4635 (4) | −2612 (3) | 4483 (1) | 1.45 (7) |
| S(2) | 952 (4) | −1454 (3) | 4311 (1) | 1.66 (7) |
| S(3) | 2822 (4) | −4306 (3) | 6202 (1) | 1.41 (7) |
| S(4) | −852 (4) | −3140 (3) | 5983 (1) | 1.49 (7) |
| S(5) | 6360 (3) | −1415 (3) | 2861 (2) | 2.23 (8) |
| S(6) | 2055 (3) | 70 (3) | 2697 (2) | 2.40 (8) |
| S(7) | 1987 (3) | −5422 (3) | 7944 (1) | 1.78 (7) |
| S(8) | −2393 (4) | −3972 (3) | 7691 (1) | 1.78 (8) |
| C(1) | 2264 (17) | −2543 (11) | 4883 (5) | 1.43 (28) |
| C(2) | 1495 (16) | −3269 (10) | 5592 (5) | 1.25 (27) |
| C(3) | 4378 (16) | −1606 (10) | 3567 (5) | 1.24 (27) |
| C(4) | 2717 (16) | −1046 (10) | 3494 (5) | 1.21 (27) |
| C(5) | 1161 (16) | −4532 (10) | 7060 (5) | 1.01 (26) |
| C(6) | −500 (16) | −3995 (10) | 6961 (5) | 0.93 (26) |
| C(7) | 6324 (17) | 358 (11) | 2403 (6) | 1.56 (29) |
| C(8) | 4066 (18) | 195 (12) | 1945 (6) | 1.94 (31) |
| C(9A) | −339 (31) | −5805 (20) | 8548 (10) | 1.5 (3)[c] |
| C(10A) | −1010 (32) | −4367 (21) | 8707 (11) | 1.8 (3)[c] |
| C(9B) | 445 (40) | −4877 (26) | 8767 (13) | 1.5 (4)[c] |
| C(10B) | −1880 (45) | −5287 (29) | 8473 (15) | 2.2 (4)[c] |

[a] The atomic parameters are taken from model I (see Tables III and IV). [b] The isotropic thermal parameters are given as $U_{equiv} = (U_{11} + U_{22} + U_{33})/3$. The anisotropic temperature factor is defined as $\exp[-2\pi(h^2U_{11} + k^2U_{22} + l^2U_{33} + 2hkU_{12} + 2hlU_{13} + 2klU_{23})]$. [c] The isotropic temperature factor is defined as $\exp[-8\pi^2B \sin^2\theta/\lambda^2]$.

all atoms in the molecule respond to the modulating wave(s) collectively. This local displacement ($\Delta\mathbf{x}$) of each atom in a rigid body can be described by three translational ($\mathbf{u}_i$) and three rotational ($\mathbf{R}_j$) vectors

$$\Delta\mathbf{x} = \sum_i \mathbf{u}_i \sin(2\pi\mathbf{q}\cdot\mathbf{g} - \phi_i) + \sum_j \mathbf{A} \times \mathbf{R}_j \sin(2\pi\mathbf{q}\cdot\mathbf{g} - \phi_j) \quad (1)$$

in which $\mathbf{g}$ is the rigid body center of mass relative to some arbitrary origin, $\phi_i$ and $\phi_j$ are the phase factors, and $\mathbf{A}$ is the atomic position relative to the center of mass. The vector $\mathbf{q}$ is the modulating wavevector such that each reflection can be described by a vector

$$\mathbf{h} = h\mathbf{a}^* + k\mathbf{b}^* + l\mathbf{c}^* + m\mathbf{q} \quad (2)$$

where the integers $h$, $k$, $l$ are the conventional Miller indices and $m$ is ±1, ±2, ±3 (etc.), corresponding to the first-, and second-, and third- (etc.) order satellite reflections.

It can be seen from eq 1 that the phase factor ($2\pi\mathbf{q}\cdot\mathbf{g}$) is of significant importance in determining the local displacements of an atom or a molecule. As $\mathbf{g}$ varies with unit cell translations, the total phase factor and the magnitudes of the atomic displacements vary from one unit cell to another.

## Experimental Section

Single crystals of $\beta$-$(ET)_2I_3$ were synthesized by electrocrystallization methods described in detail elsewhere.[16] A black, single crystal (approximate dimensions 0.13 × 0.15 × 0.15 mm) was selected for X-ray diffraction data collection, conducted on a Syntex $P2_1$ automatic four-circle diffractometer using Mo K$\alpha$ radiation. The temperature of the crystal was maintained at 120 (5) K with use of a locally constructed nitrogen-gas flow system. The unit cell dimensions given in Table I were determined from the setting angles of 25 fundamental Bragg reflections selected in the $2\theta$ range of 33–37°. The vector $\mathbf{q}$, as defined in eq 2, was determined from the setting angles of 22 additional first-order satellite reflections to be $[0.076\ (2)]\mathbf{a}^* + [0.272\ (4)]\mathbf{b}^* + [0.206\ (3)]\mathbf{c}^*$.

During data collection, the intensities of two Bragg reflections were monitored after every 94 reflections measured, and no significant change of their intensities was observed throughout the experiment. The data collection routine was modified such that the intensities of both the fundamental and satellite reflections were measured. Details of the intensity data collection and reductions are summarized in Table I.

The basic crystal structure was first refined by using only the fundamental Bragg reflection data. The initial non-hydrogen atomic parameters were taken from the room-temperature structure determination.[16] The atomic scattering factors and anomalous dispersion terms for I, S, and C were taken from the International Tables for X-ray Crystallography.[33] The quantity minimized in the least-squares refinement was $\sum w(|F_o| - |F_c|)^2$ with weights $w = 1/\sigma^2(F_o)$ and $\sigma = [\sigma_c^2 + (0.02F_o)^2]^{1/2}$. The refined occupancy factors of the disordered ethylene group C atoms of the ET molecule [C(9A)–C(10A) as group "A" and C(9B)–C(10B) as group "B", see Table II] averaged to 0.56 (3) and 0.44 (3) for the A and B groups, respectively.

**Table III.** Least-Squares Refinement Results of the Modulated Structure of $\beta$-$(ET)_2I_3$[a]

| | model I | model II |
|---|---|---|
| fundamental reflections | | |
| $R(F)$ | 0.042 | 0.043 |
| $R(wF)$ | 0.067 | 0.066 |
| goodness of fit | 2.42 | 2.42 |
| NO[b] | 2516 | 2516 |
| NV | 177 | 179 |
| satellite reflections | | |
| $R(F)$ | 0.126 | 0.117 |
| $R(wF)$ | 0.165 | 0.141 |
| goodness of fit | 4.94 | 4.25 |
| NO[b] | 2758 | 2758 |
| NV | 21 | 33 |
| combined | | |
| $R(F)$ | 0.071 | 0.067 |
| $R(wF)$ | 0.119 | 0.105 |
| goodness of fit | 4.02 | 3.55 |
| NO[b] | 5274 | 5274 |
| NV | 198 | 212 |

[a] Reflections for which $F_o > 3\sigma(F_o)$(fundamental) or $F_o > 10\sigma(F_o)$(satellite) were used in the least-squares refinement. [b] NO and NV are the number of observations (independent reflections) and the number of variables, respectively, used in the least-squares analysis.

The modulated structure was further refined by using both fundamental and satellite reflection data (see Table III for details). The least-squares refinement procedure used here is described elsewhere.[32,34] The atomic positional and thermal parameters are given in Table II, and the rigid-body displacive parameters are presented in Table IV. The interatomic distances and angles are summarized in Tables V and VI.

Two different models were used to describe the modulated structure of $\beta$-$(ET)_2I_3$. In model I, the rigid-body displacive modulations consisted of translational displacements for I(1) and I(2) and of translational and rotational displacements for the ET molecules (see Table IV). Since the linear $I_3^-$ anion resides at a center of symmetry in the lattice, it is defined by only two different I atom positions [I(1) and I(2)]. Separate translational displacements for each I atom in the triiodide anion were used in order to simulate the rotational displacement and internal distortion of the $I_3^-$ anion.

The residual density map was calculated by a Fourier synthesis, based on the refined atomic parameters of the I, S, and C atoms. The largest features were the residual densities of the I atoms. All the hydrogen positions were located and were observed to be close to the calculated positions assuming $sp^3$-hybridized carbon atoms and a C–H distance of 1.08 Å. As a result of the systematic errors inherent in the X-ray determined hydrogen atom positions (0.1–0.2 Å),[35] the calculated positions of the hydrogen atoms were used in the subsequent calculations of distances and angles.

A detailed analysis of the intermolecular contacts (see Discussion) suggested that the occupancy factors of the disordered ethylene group [A and B groups for C(9)–C(10); see Figure 1] might be correlated to the structural modulation. Hence, a second model (Model II in Table IV) was used in order to *simulate* the modulation of the site occupancy factors. In this model, independent carbon atoms [C(9) and C(10)] were initially placed at their average positions and their translational displacements were refined independently (see Table IV). The "local" positions of C(9) and C(10) as calculated from eq 1 were used to model the modulations of the disordered A and B site occupancy factors (see Discussion), such that the "local" carbon atom positions account for the electron densities of the ethylene groups at the respective A and B sites in different unit cells. For example, to simulate the presence of the ethylene group at the A site, the displacements of C(9) and C(10) are

(33) "International Tables for X-ray Crystallography"; Knoch Press: Birmingham, England, 1974; Vol. IV.
(34) The computer program JANA used in this least-squares analysis was written by V. Petricek and P. Coppens.[32]
(35) Bacon, G. E. "Neutron Scattering in Chemistry"; Butterworths: London, 1977; p 80.

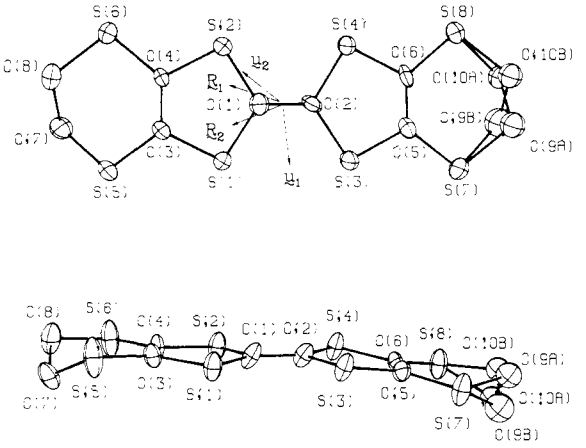

**Figure 1.** The molecular geometry of BEDT-TTF with the atomic labeling scheme. The arrows indicate the directions of the displacive vectors (arbitrary lengths) for the BEDT-TTF molecule. The rotational vectors ($\mathbf{R}_1$ and $\mathbf{R}_2$) and the translational vector ($\mathbf{u}_2$) are slightly out of the molecular plane (see text).

directed such that they are closer to it. It should be noticed that the displacive parameters of C(9) and C(10) were used specifically to describe the occupational modulation of the disordered ethylene sites. They are, in fact, a poor description of the geometry of this ethylene group.

A comparison of the agreement factors (see Table III) indicates that model II accounts for the observed structure factors somewhat better than model I. While model II describes the modulations of the site occupancy factors of the disordered ethylene group, model I assumes a random distribution of the two disordered sites. However, the interatomic distances are more meaningful in model I. Hence all subsequent discussions on crystal packing and interatomic distances and angles are based on model I.

## Discussion

**"Average" Crystal and Molecular Structures.** The ET molecule in $\beta$-$(ET)_2I_3$ is nearly planar [see Figure 1 and Table X2 (supplementary material)] for the fulvalene portion of the molecule, with large deviations from planarity for the terminal ethylene groups. An important feature is the *disordered* ethylene group [C(9A)–C(10A) and C(9B)–C(10B) of Figure 1—designated as A and B groups] at one end of the ET molecule and the *ordered* group at the opposite end [C(7)–C(8)—designated as the C group]. The present analysis shows that the interactions of the disordered ethylene group with the surrounding triiodide ions are responsible for the unusual structural modulation in $\beta$-$(ET)_2I_3$ (vide infra). The formal charge of +0.5 $e^-$ of each ET molecule, as determined by the stoichiometry, is in good agreement with recently developed correlations between the intramolecular bond lengths and the charge on the radical cation.[11]

As mentioned previously, the ET molecules form infinite columns along the [110] direction which also pack in a side-by-side fashion to form a 2-D "corrugated sheet" network on the *ab* plane.[16] As suggested by the *intra*stack S···S distances, which are always *larger* than their van der Waal radii sum (3.60 Å), the ET molecules are considered to be loosely connected along the columns. Short *inter*stack S···S contacts which are significantly less than 3.60 Å are observed between adjacent columns (see Table VI and Figures 2 and 3). The *inter*stack interactions between adjacent ET molecules extend along the [100] and [$\bar{1}$10] directions.

The crystal packing of the ET molecules in $\beta$-$(ET)_2I_3$ is in sharp contrast to the crystal packing motif of the 1-D conducting $(TMTSF)_2X$ (X = $ClO_4^-$, $BF_4^-$, $PF_6^-$, $AsF_6^-$, etc.) salts.[7] In the

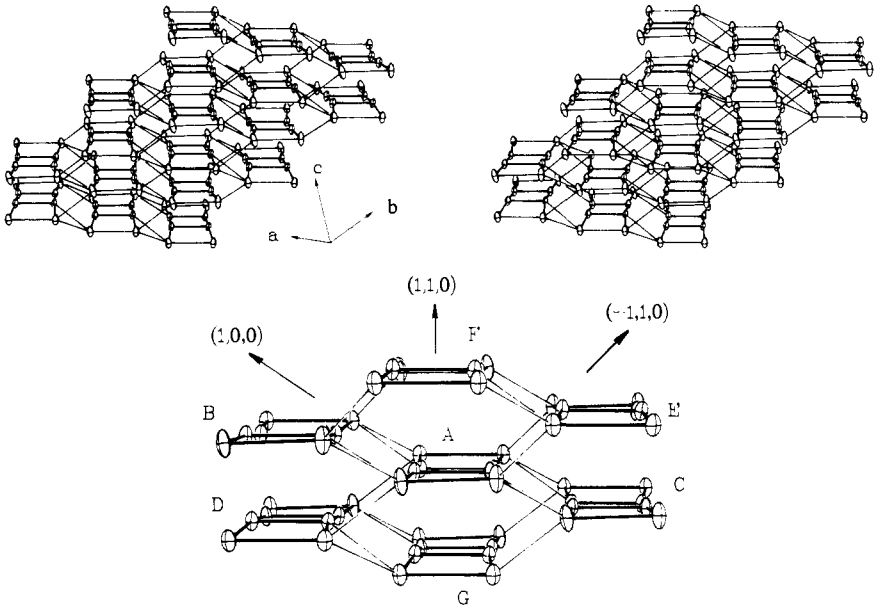


**Figure 2.** (a, top) Stereoview of the 2-D network of the BEDT-TTF molecules. For clarity, only the S atoms in the BEDT-TTF molecules are shown. Significant intermolecular *inter*stack S···S contacts (<3.6 Å) are indicated by the thin lines. (b, bottom) An enlarged portion of the 2-D network. The approximate intermolecular directions with respect to the cell axes are indicated. The symmetry operations which relate the molecules are A ($x,y,z$), B ($1+x,y,z$), C ($x-1,y,z$), D ($1-x,-y-1,1-z$), E ($-x,-y,1-z$), F ($1-x,-y,1-z$), and G ($-x,-1-y,1-z$).

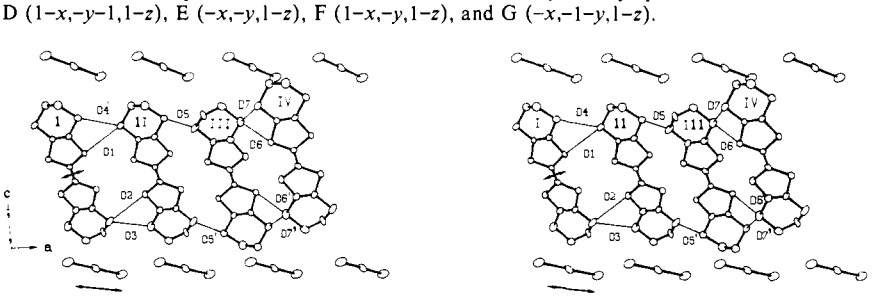

**Figure 3.** Stereoview of the intermolecular contacts between adjacent BEDT-TTF molecules in $\beta$-$(BEDT\text{-}TTF)_2I_3$. The arrows indicate the directions of the major components of the displacive vectors for the BEDT-TTF molecules and $I_3^-$ anions.

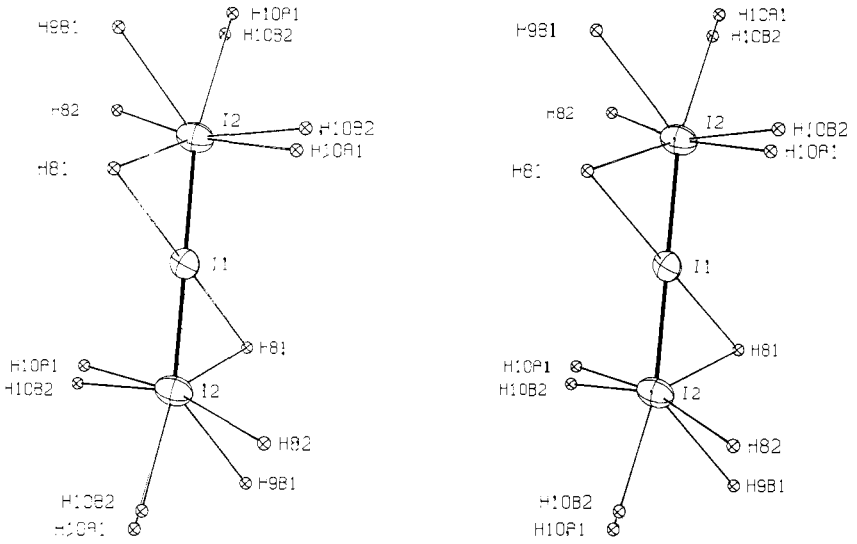


**Figure 4.** Stereoview of the environment of the triiodide anion. Short H···I contacts (<3.3 Å) are indicated by thin lines. The hydrogen atom ellipsoids are on an arbitrary scale. The calculated hydrogen positions were used (see Experimental Section).

$(TMTSF)_2X$ salts, the *intra*stack interactions are observed to be very significant and have Se···Se distances equal to or less than those along the *inter*stack directions.[36,37] The differences in the packing motif of the two radical cations are reflected in the electronic properties of these salts: $\beta$-$(ET)_2I_3$ is a two-dimensional electrical conductor[14,38] and the $(TMTSF)_2X$ salts have a rather one-dimensional electronic structure[39] and electrical conductivity.[7]

Along the columns of triiodide anions, the adjacent terminal I atoms are at van der Waal contact distances [d(I···I) = 4.20 Å] and are along the [110] direction. These anion columns are located between the "sheets" of ET molecules and alternate with the latter along the *c* axis. The short H···I distances given in Table VI indicate possible C—H···I interactions (see Figure 4). Some of these short interatomic distances are smaller than the sum of their respective van der Waal radii [$R_{vdw}(H) + R_{vdw}(I)$ = 3.2–3.6 Å].[40] Such short H···I distances are very common in crystals containing polyiodide ions[41] and appear to contribute significantly to the overall crystal packing forces.

**The Modulated Structure.** The displacement vectors for the triiodide ion and the ET molecules are different in direction and magnitude and are summarized in Table IV and illustrated in Figures 1 and 3. The major component of the $I_3^-$ anion displacement is along the [100] direction with an amplitude of ~0.27 Å. For the ET molecule, the major component is nearly perpendicular to the column axis, [110], and is in the molecular plane. The displacement amplitude (~0.11 Å) for the ET molecule is considerably smaller than that of the $I_3^-$ ion. Because of the structural modulation, the unit cell translational symmetries in the average structure are no longer valid. A highly significant finding is that the intermolecular atomic distances *fluctuate* from one "unit cell" to the other. Since the atomic positions vary sinusoidally about their respective average values, the interatomic distances vary periodically, also. The variations of the interstack S···S contact distances are summarized in Table VI and Figures 2 and 5.

While the local fluctuations of the interstack S···S contact distances between adjacent ET molecules are significant, the 2-D network remains intact throughout the crystal. This is because the modulation of those distances in the approximate direction [$\bar{1}$10] (see molecules A and E in Figure 2b and D5 and D5′ in Table VI) is out of phase with that in each of the directions [100] (A–B; D1′–D4′), [$\bar{1}$00] (A–C; D1–D4), and [1$\bar{1}$0] (A–D; D7 and D7′).[42] In addition, the distances between the ET pairs A–B, A–C, and A–D are approximately in phase. The phase relationship between these sets of S···S contact distances is presented in Figure 5. These phase relationships hold for any directions in the *ab* plane, although the periodicity of the modulation varies with the directions. The period of modulation is the projection of the wavevector, **q**, on the direction of propagation. Consequently, in spite of the significant local fluctuations of the interstack S···S distances, the 2-D nature of the structure is preserved. It is also expected that the overall intermolecular overlap between the ET molecules in the 2-D network remains unchanged.

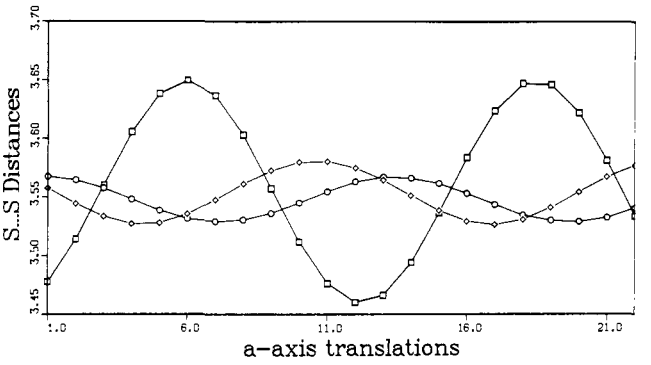


**Figure 5.** A plot of the variations of interstack S···S contacts vs. unit cell translations along the *a* axis: (◇) average values of D1–D4; (○) average values of D5 and D5′; and (□) average values of D7 and D7′ (see Table VI).

**Structure–Property Relations.** The 2-D networks of the ET molecules in the charge-transfer salts $\beta$-$(ET)_2I_3$[13–17] and $(ET)_2ClO_4(TCE)_{0.5}$[18,43] have been shown to be closely related to their electrical properties. It has been suggested that as a consequence of the highly developed 2-D network of the ET molecules, the MI transition does not occur in these materials. In contrast, all but one of the $(TMTSF)_2X$ salts[44] and the more familiar

(36) Flandrois, S.; Coulon, C.; Delhaes, P.; Chasseau, D.; Hauw, C.; Gaultier, J.; Fabre, J. M.; Giral, L. *Mol. Cryst. Liq. Cryst.* **1982**, *79*, 307.
(37) Beno, M. A.; Blackman, G. S.; Williams, J. M.; Bechgaard, K. *Inorg. Chem.* **1982**, *21*, 3860.
(38) Mori, T.; Kobayashi, A.; Sasaki, Y.; Kobayashi, H.; Saito, G.; Inokuchi, H. *Chem. Lett.* **1984**, 957.
(39) Whangbo, M. H.; Williams, J. M.; Beno, M. A.; Dorfman, J. R. *J. Am. Chem. Soc.* **1983**, *105*, 645.
(40) Huheey, J. E. "Inorganic Chemistry: Principles of Structure and Reactivity"; Harper: New York, 1972; p 184.
(41) Coppens, P. In "Extended Linear Chain Compounds"; Miller, J. S., Plenum Press: New York, 1982; p 333.
(42) The distinction between S···S contacts D5 and D5′ etc. is a result of the phase differences between the rotational displacive modulations of adjacent ET molecules.
(43) Kobayashi, H.; Kobayashi, A.; Sasaki, Y.; Saito, G.; Enoki, T.; Inokuchi, H. *J. Am. Chem. Soc.* **1984**, *105*, 297.
(44) Bechgaard, K.; Jacobsen, C. S.; Mortensen, K.; Pedersen, H. J.; Thorup, N. *Solid State Commun.* **1980**, *33*, 1119.

**Table IV.** Rigid-Body Modulation Parameters[a]

| | | model I | model II |
|---|---|---|---|
| $\mathbf{u}_1$ [I(1)] | $u_x$ | 0.0394 (2) | 0.0396 (2) |
| | $u_y$ | 0.0008 (2) | 0.0008 (1) |
| | $u_z$ | −0.0038 (1) | −0.0038 (1) |
| | $\phi$, deg | 0 | 0 |
| | $\|u\|$, Å | 0.268 (2) | 0.270 (1) |
| $\mathbf{u}_1$ [I(2)] | $u_x$ | 0.0431 (2) | 0.0429 (2) |
| | $u_y$ | 0.0021 (1) | 0.0022 (1) |
| | $u_z$ | −0.0003 (1) | −0.0003 (1) |
| | $\phi$, deg | 0 | 0 |
| | $\|u\|$, Å | 0.277 (1) | 0.276 (1) |
| $\mathbf{u}_2$ [I(2)] | $u_x$ | −0.0035 (2) | −0.0038 (2) |
| | $u_y$ | 0.0074 (1) | 0.0072 (1) |
| | $u_z$ | 0.0029 (1) | 0.0029 (1) |
| | $\phi$, deg | −90 | −90 |
| | $\|u\|$, Å | 0.088 (1) | 0.087 (1) |
| $\mathbf{u}_1$ [ET] | $u_x$ | 0.0141 (2) | 0.0147 (2) |
| | $u_y$ | −0.0043 (1) | −0.0041 (1) |
| | $u_z$ | 0.0014 (1) | 0.0014 (1) |
| | $\phi$, deg | 0 | 0 |
| | $\|u\|$, Å | 0.113 (1) | 0.115 (1) |
| $\mathbf{u}_2$ [ET] | $u_x$ | −0.0015 (2) | −0.0014 (2) |
| | $u_y$ | 0.0022 (1) | 0.0014 (1) |
| | $u_z$ | −0.0021 (1) | −0.0022 (1) |
| | $\phi$, deg | −90 | −90 |
| | $\|u\|$, Å | 0.041 (1) | 0.038 (1) |
| $\mathbf{R}_1$ [ET] | $R_x$ | 0.0004 (1) | 0.0004 (1) |
| | $R_y$ | 0.0012 (1) | 0.0012 (1) |
| | $R_z$ | −0.0006 (1) | −0.0006 (1) |
| | $\phi$, deg | 0 | 0 |
| | $\|R\|$, deg | 0.838 (1) | 0.841 (1) |
| $\mathbf{R}_2$ [ET] | $R_x$ | 0.0024 (1) | 0.0023 (1) |
| | $R_y$ | 0.0013 (1) | 0.0013 (1) |
| | $R_z$ | −0.0004 (1) | −0.0004 (1) |
| | $\phi$, deg | −90 | −90 |
| | $\|R\|$, deg | 1.034 (1) | 1.010 (1) |
| $\mathbf{u}_1$ [C(9)] | $u_x$ | | −0.0029 (30) |
| | $u_y$ | | 0.0157 (25) |
| | $u_z$ | | 0.0012 (10) |
| | $\phi$, deg | | 180 |
| | $\|u\|$, Å | | 0.149 (24) |
| $\mathbf{u}_2$ [C(9)] | $u_x$ | | 0.0556 (25) |
| | $u_y$ | | 0.0720 (17) |
| | $u_z$ | | 0.0166 (8) |
| | $\phi$, deg | | −90 |
| | $\|u\|$, deg | | 0.637 (13) |
| $\mathbf{u}_1$ [C(10)] | $u_x$ | | 0.0205 (32) |
| | $u_y$ | | 0.0084 (23) |
| | $u_z$ | | 0.0038 (10) |
| | $\phi$, deg | | 0 |
| | $\|u\|$, Å | | 0.133 (17) |
| $\mathbf{u}_2$ [C(10)] | $u_x$ | | 0.0678 (29) |
| | $u_y$ | | 0.0592 (19) |
| | $u_z$ | | 0.0172 (9) |
| | $\phi$, deg | | 90 |
| | $\|u\|$, Å | | 0.581 (14) |

[a] Each displacive vector is represented in fractional coordinates such that $\mathbf{u} = u_x\mathbf{a} + u_y\mathbf{b} + u_z\mathbf{c}$ and $\mathbf{R} = R_x\mathbf{a} + R_y\mathbf{b} + R_z\mathbf{c}$. $\phi$ is the phase angle given for each displacive vector and is defined in eq 1. $|u|$ and $|R|$ are the magnitudes of the translations and rotational vectors, respectively.

TTF-TCNQ salt,[24] which have been characterized as 1-D systems, undergo MI transitions at low temperatures and ambient pressure. The two-dimensional nature of the ET molecular network is particularly important in $\beta$-$(ET)_2I_3$ below $T = 195$ K. Because of the structural modulation, the local fluctuations of interstack S···S contacts are significant (see Table VI and Figure 5), thereby modifying the magnitudes of the overlaps between the ET molecules. However, it has been shown in this study that the network of the ET molecules in $\beta$-$(ET)_2I_3$ remains intact and the overall intermolecular interactions are preserved only because of its 2-D nature. Such local modifications of the intermolecular contacts of comparable magnitudes ($\simeq\pm0.1$ Å) have been observed in the $(TMTSF)_2ReO_4$[45] and $(TMTSF)_2BF_4$[46] salts, as results of commensurate crystallographic phase transitions. These latter crystallographic phase transitions are closely related to the MI and order–disorder transitions observed in these materials.[45-48] In contrast, the metallic properties of $\beta$-$(ET)_2I_3$ are *preserved* in spite of the incommensurate phase transition.[20] The electrical conductivity of this material increases fairly smoothly with decreasing temperature through the incommensurate phase transition at about 195 K.

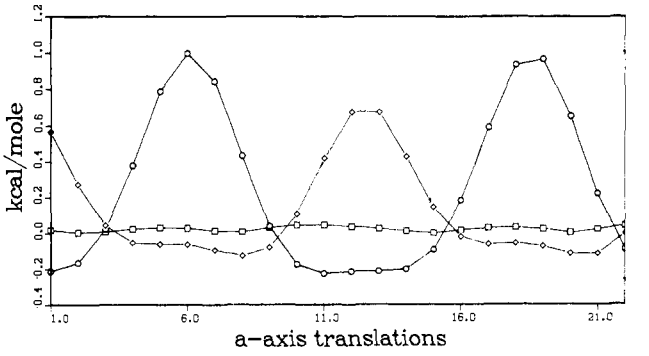


**Figure 6.** A plot of the variations of the ethylene group site potentials vs. unit cell translations along the *a* axis: (◇) (disordered) A group, (○) (disordered) B group, and (□) (ordered) C group.

**Origin of the Structural Phase Transition.** In this section, it will be shown that the driving forces of the structural modulation originate from anion–cation interactions. In particular, an ET molecule with the A or B disordered ethylene groups leads to unfavorable H···I contacts which suggests preferential site occupanices in the modulated structure (see Table VI and Figure 4).

In an attempt to analyze these interactions between the counterions, the site potential of each ethylene group has been calculated. The pairwise energy ($\phi$) of the H···I interaction has been previously described by the use of an empirical equation[41]

$$\phi(r) = 3.813 \times 10^4 \exp(-3.61r) - 589r^{-6} \text{ kcal/mol} \quad (3)$$

in which $r$ is the H···I distance which varies with unit cell translations. In corresponding fashion, the site potential [$V(\mathbf{t})$] of an ethylene group in the $\beta$-$(ET)_2I_3$ structure is

$$V(\mathbf{t}) = \sum_{H_i} \sum_{I_j} \phi_{ij}(r) \quad (4)$$

where the double summations are over all $H_i$ in an ethylene group and all $I_j$ less than 3.9 Å from $H_i$ (arbitrary cutoff value); t is the unit cell translation in the average structure. As a result of the structural modulation in $\beta$-$(ET)_2I_3$, this site potential varies from one unit cell to the next. These variations are summarized in Figure 6 for the ordered (C) and disordered (A and B) ethylene groups. The site potential of the C group is observed to remain constant throughout the crystal, while those of the disordered A and B groups vary substantially and are out of phase with each other. The site-potential variations of the disordered ethylene group suggest that there can be preferential occupancies among the two disordered sites in the crystal such that the energies of H···I interactions can be minimized when one site is selected over the other. In other words, the occupancies of these two disordered sites, which are *random* at higher temperature, become *correlated*

(45) Rindorf, G.; Soling, H.; Thorup, N. *Acta Crystallogr., Sect. C* **1984**, *C40*, 1137.
(46) Emge, T. J.; Williams, J. M.; Leung, P. C. W.; Schultz, A. J.; Beno, M. A.; Wang, H. H. *Mol. Cryst. Liq. Cryst.* **1985**, *119*, 237.
(47) Jacobsen, C. S.; Pedersen, H. J.; Mortensen, K.; Rindorf, G.; Thorup, N.; Torrance, J. B.; Bechgaard, K. *J. Phys. C.: Solid State Phys.* **1982**, *15*, 2651.
(48) Moret, R.; Pouget, J. P.; Comes, R.; Bechgaard, K. *Phys. Rev. Lett.* **1982**, *49*, 1008.

**Table V.** Interatomic Distances (Å) and Angles (deg) for $\beta$-$(ET)_2I_3$

| | | | | | |
|---|---|---|---|---|---|
| I(1)–I(2) | 2.904 (1) | S(5)–C(3) | 1.742 (9) | C(1)–C(2) | 1.350 (12) |
| | | S(6)–C(4) | 1.753 (8) | | |
| S(1)–C(1) | 1.746 (10) | S(7)–C(5) | 1.754 (8) | C(3)–C(4) | 1.350 (12) |
| S(2)–C(1) | 1.744 (9) | S(8)–C(6) | 1.752 (9) | C(5)–C(6) | 1.338 (12) |
| S(3)–C(2) | 1.742 (8) | S(5)–C(7) | 1.806 (9) | | |
| S(4)–C(2) | 1.744 (9) | S(6)–C(8) | 1.812 (10) | C(7)–C(8) | 1.522 (15) |
| | | S(7)–C(9A) | 1.808 (18) | C(9A)–C(10A) | 1.514 (22) |
| S(1)–C(3) | 1.749 (8) | S(7)–C(9B) | 1.822 (21) | C(9B)–C(10B) | 1.451 (37) |
| S(2)–C(4) | 1.759 (9) | S(8)–C(10A) | 1.831 (17) | | |
| S(3)–C(5) | 1.764 (9) | S(8)–C(10B) | 1.834 (23) | | |
| S(4)–C(6) | 1.762 (8) | | | | |
| | | | | | |
| C(1)–S(1)–C(3) | 95.4 (4) | S(1)–C(1)–S(2) | 115.0 (5) | S(5)–C(3)–C(4) | 127.5 (6) |
| C(1)–S(2)–C(4) | 95.3 (4) | S(3)–C(2)–S(4) | 115.4 (5) | S(6)–C(4)–C(3) | 129.2 (7) |
| C(2)–S(3)–C(5) | 95.0 (4) | | | S(7)–C(5)–C(6) | 129.2 (6) |
| C(2)–S(4)–C(6) | 94.9 (4) | S(1)–C(1)–C(2) | 122.9 (7) | S(8)–C(6)–C(5) | 128.9 (6) |
| | | S(2)–C(1)–C(2) | 122.1 (7) | | |
| C(3)–S(5)–C(7) | 99.6 (4) | S(3)–C(2)–C(1) | 123.1 (7) | S(5)–C(7)–C(8) | 113.2 (7) |
| C(4)–S(6)–C(8) | 102.8 (4) | S(4)–C(2)–C(1) | 121.4 (7) | S(6)–C(8)–C(7) | 114.4 (6) |
| C(5)–S(7)–C(9A) | 100.6 (6) | S(1)–C(3)–S(5) | 115.3 (5) | S(7)–C(9A)–C(10A) | 112.8 (12) |
| C(5)–S(7)–C(9B) | 98.2 (7) | S(2)–C(4)–S(6) | 114.0 (5) | S(7)–C(9B)–C(10B) | 115.7 (15) |
| C(6)–S(8)–C(10A) | 99.6 (6) | S(3)–C(5)–S(7) | 113.8 (5) | S(8)–C(10A)–C(9A) | 112.8 (11) |
| C(6)–S(8)–C(10B) | 100.5 (8) | S(4)–C(6)–S(8) | 113.8 (5) | S(8)–C(10B)–C(9B) | 111.9 (17) |
| | | | | | |
| | | S(1)–C(3)–C(4) | 117.2 (6) | I(2)–I(1)–I(2′) | 180.0 |
| | | S(2)–C(4)–C(5) | 116.8 (6) | | |
| | | S(3)–C(5)–C(6) | 117.0 (6) | | |
| | | S(4)–C(6)–C(7) | 117.3 (6) | | |

**Table VI.** Selected Intermolecular Contact Distances for $\beta$-$(ET)_2I_3$

| contacts | average[b] | 120 K range (max – min) | Δ[d] | 298 K | symmetry (2nd atom) |
|---|---|---|---|---|---|
| | | (A) Intermolecular Distances | | | |
| I(2)–I(2) | 4.195 (2) | 4.149–4.309 | 0.150 | 4.211 (1) | a[a] |
| interstack S–S distances | | | | | |
| D1 S(3)–S(8) | 3.578 (3) | 3.553–3.604 | 0.051 | 3.651 (2) | b |
| D2 S(5)–S(2) | 3.553 (4) | 3.520–3.587 | 0.067 | 3.574 (2) | b |
| D3 S(5)–S(6) | 3.550 (4) | 3.502–3.598 | 0.096 | 3.600 (2) | b |
| D4 S(7)–S(8) | 3.533 (4) | 3.511–3.556 | 0.045 | 3.598 (2) | b |
| D5 S(5)–S(7) | 3.547 (3) | 3.516–3.580 | 0.064 | 3.628 (2) | c |
| D6 S(4)–S(6) | 3.626 (3) | 3.609–3.643 | 0.034 | 3.691 (2) | d |
| D7 S(6)–S(8) | 3.552 (3) | 3.458–3.652 | 0.197 | 3.593 (2) | d |
| intrastack S–S distances | | | | | |
| S(1)–S(4) | 3.725 (4) | 3.687–3.763 | 0.076 | | e |
| S(2)–S(3) | 3.722 (3) | 3.703–3.741 | 0.038 | | e |
| S(3)–S(4) | 3.695 (3) | 3.678–3.714 | 0.036 | | e |
| | | (B) H–I Contact Distances[c] | | | |
| H(71)–I(2) | 3.46 | 3.43–3.51 | 0.08 | | f |
| H(71)–I(1) | 3.60 | 3.43–3.76 | 0.33 | | b |
| H(81)–I(2) | 3.05 | 2.99–3.12 | 0.03 | | g |
| H81)–I(1) | 3.30 | 3.27–3.33 | 0.06 | | g |
| H(82)–I(2) | 3.21 | 3.11–3.30 | 0.19 | | f |
| H(82)–I(1) | 3.35 | 3.30–3.41 | 0.11 | | g |
| H(9A1)–I(2) | 3.35 | 3.23–3.48 | 0.25 | | h |
| H(10A1)–I(2) | 3.00 | 2.73–3.28 | 0.55 | | d |
| H(10A1)–I(2) | 3.21 | 3.01–3.41 | 0.40 | | i |
| H(10A2)–I(1) | 3.39 | 3.21–3.58 | 0.37 | | j |
| H(9B1)–I(2) | 3.23 | 2.97–3.52 | 0.55 | | k |
| H(9B2)–I(2) | 3.44 | 3.34–3.54 | 0.20 | | h |
| H(9B2)–I(2) | 3.58 | 3.42–3.78 | 0.36 | | k |
| H(10B1)–I(2) | 3.49 | 3.31–3.69 | 0.37 | | i |
| H(10B2)–I(2) | 2.83 | 2.64–3.03 | 0.39 | | i |
| H(10B2)–I(2) | 3.29 | 3.04–3.54 | 0.50 | | d |

[a] The symmetry operations of the second atom in each pair are the following: (a) $1-x, 1-y, -z$; (b) $1+x, y, z$; (c) $1+x, -1-y, 1-z$; (d) $-x, -y, 1-z$; (e) $-x, -1-y, 1-z$; (f) $1-x, -y, -z$; (g) $x, y, z$; (h) $x, y-1, 1+z$; (i) $x-1, y-1, 1+z$; (j) $x, y, 1+z$; and (k) $1-x, -y, 1-z$. [b] The average structure refers to the refined atomic parameters using both fundamental and satellite reflections. These atomic distances are affected by the sinusoidal modulation resulting in a range of distances which are calculated with eq 1. [c] All hydrogen positions are calculated by using idealized $sp^3$ hybridized carbon geometries and a C–H distance of 1.08 Å, therefore, no esd's are given. [d] Δ is the difference between the maximum and minimum values.

below the transition temperature of ~195 K in the incommensurate superlattice.

In order to simulate this occupational modulation, an alternate model (model II) was used in which the C atoms in the disordered ethylene group were placed at their respective averaged positions [C(9) and C(10)]. These two "atoms" were allowed to modulate independently. The unit-cell dependent local coordinates of C(9) and C(10) were calculated by using their respective displacive parameters (see Table IV) in eq 1. These displacements correlate very well with the site-potential distributions of the disordered

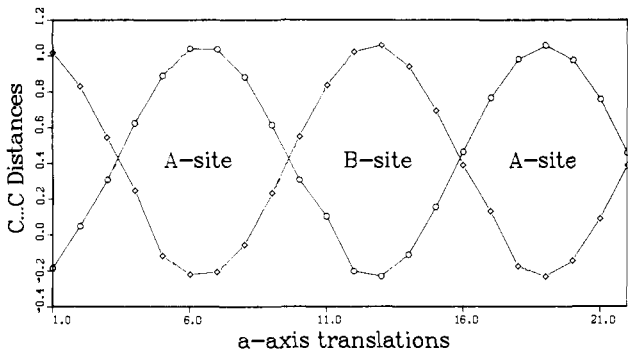


**Figure 7.** Variation of the ethylene group configurations (A or B) as a function of the unit cell translations along the *a* axis. The C···C distances (◇) C(9)–C(9A) and (○) C(9)–C(9B) are the calculated distances of each carbon atom from the respective A or B site. The variations of C(10)–C(10A) and C(10)–C(10B) distances are nearly identical with those given in this figure. A negative distance indicates that the calculated carbon position is outside of the region between the A and B sites. The *preferred* sites, based on packing arguments (A or B), are also indicated.

ethylene group (A and B sites) given in Figure 6, in that the positional shifts of C(9) and C(10) follow the lower of the two potential distributions. Relative to some arbitrary origin for the unit cell translations, in unit cells 4 to 9, for example, these carbon atoms occupy the A site, and in unit cells 10 to 15 they occupy the B site (see Figure 7).

Therefore, the local positions of the ET molecules, and the intermolecular overlaps between them, vary in concert with the H···I interactions. A detailed analysis indicates that the local displacements of the ET molecule and triiodide ions correlate with the site occupancies of the disordered ethylene group such that very short H···I contacts [e.g., H(10A1)···I(2) (2.73 Å) and H(10B2)···I(2) (2.64 Å)] are avoided. However, the network of intermolecular interactions between the cations is preserved as a result of its 2-D nature (vide supra).

In the light of the very important cation–anion (C—H···I) packing interactions, the intercation interactions probably do not contribute significantly to the driving forces of the structural modulation. In the isostructural $\beta$-$(ET)_2IBr_2$ superconductor[49] and $\beta$-$(ET)_2I_2Br$ conductor,[50] nearly identical packing of the ET molecules has been observed. However, no structural modulation is observed in either system down to a temperature of 120 K, probably because of the size differences of the $I_3^-$, $I_2Br^-$, and $IBr_2^-$ anions. The molecular dimensions (sum of two bond lengths) of these linear anions are ~5.8,[50] 5.6,[50] and 5.4 Å[49] for the $I_3^-$, $I_2Br^-$, and $IBr_2^-$ anions, respectively. Hence, the differences of 0.4–0.2 Å among these anions are very significant and are sufficient to change the nature of H···X (X = I or Br) interactions in the $\beta$-$(ET)_2X_3$ salts. As a result, the ethylene groups in the ET molecules are observed to be *ordered* in $\beta$-$(ET)_2IBr_2$ and $\beta$-$(ET)_2I_2Br$ at 120 K and only the B-site is occupied in each case.

## Conclusion

It has been shown that the low-temperature incommensurate modulation of the crystal structure of the ambient pressure organic superconductor $\beta$-$(ET)_2I_3$ has no drastic effects on the electrical properties of this material.[20] In spite of the incommensurate phase transition at 195 K, the metallic state of this material is preserved and the onset of superconductivity occurs at $T_c \simeq 1.4$ K. It has been shown in the present study that the two-dimensional nature of the intermolecular interactions between the organic molecules is also preserved regardless of the structural modulation. In view of the present structural analysis, the origin of the structural modulation appears to be the anion–cation ($I\cdots H_2C-$) interactions. Also, it appears that neither the A nor B configurations of the disordered ethylene group in $\beta$-$(ET)_2I_3$ *alone* can accommodate all possible interactions with the triiodide anions. As both configurations would involve unfavorable H···I contacts, a combination of the two configurations in a modulated fashion is required to achieve a favorable packing arrangement in the crystal. The structural modulation in $\beta$-$(ET)_2I_3$ persists down to at least 8 K[51] while the modulation wavevector, **q**, remains constant throughout the temperature range. Thus, it appears likely that this structural modulation and superconductivity may co-exist at low temperatures ($T < 1.4$ K). This may then be the first example of such a phenomenon in an organic radical–cation system. Previous studies of $(TMTSF)_2ClO_4$ indicated that long-range ordering of molecular packing is also a prerequisite for superconductivity.[52] In $\beta$-$(ET)_2I_3$, this long-range ordering is accomplished by means of a structural modulation at $T < 200$ K.

**Acknowledgment.** Work at Argonne National Laboratory was supported by the Office of Basic Energy Sciences, Division of Material Sciences, of the U.S. Department of Energy, under Contract W-31-109-Eng-38.

**Supplementary Material Available:** Tables of atomic positional, including calculated hydrogen atom positions, and anisotropic thermal parameters (Table X1), molecular least-squares plane (Table X2), and a listing of observed and calculated structure factors (27 pages). Ordering information is given on any current masthead page.

(49) Williams, J. M.; Wang, H. H.; Beno, M. A.; Emge, T. J.; Sowa, L. M.; Copps, T. J.; Behroozi, F.; Hall, L. H.; Carlson, K. D.; Crabtree, G. W. *Inorg. Chem.* **1984**, *23*, 3839.

(50) Emge, T. J.; Wang, H. H.; Beno, M. A.; Leung, P. C. W.; Firestone, M. A.; Jenkins, H. C.; Cook, J. D.; Carlson, K. D.; Williams, J. M.; Venturini, E. L.; Azevedo, L. J.; Schirber, J. E. *Inorg. Chem.* **1985**, *24*, 1736.

(51) Beno, M. A.; Emge, T. J.; Leung, P. C. W.; Wang, H. H.; Sowa, L. M.; Williams, J. M., work in progress (1985).

(52) Pouget, J. P.; Shirane, G.; Bechgaard, K.; Fabre, J. M. *Phys. Rev. B: Condens. Matter* **1983**, *B27*, 5203.

(53) Permanent Address: Institute of Physics, Czechoslovak Academy of Sciences, Praha, Czechoslovakia.